

# Influence of the disorder on tracer dispersion in a flow channel

V. J. Charette <sup>1</sup>, E. Evangelista <sup>1</sup>, R. Chertcoff <sup>1</sup>, H. Auradou <sup>2</sup>, J. P. Hulin <sup>2</sup> and I. Ippolito <sup>1</sup>

<sup>1</sup>*Grupo de Medios Porosos, Facultad de Ingeniería, Universidad de Buenos Aires, Paseo Colón 850, 1063 Buenos Aires, Argentina. and*

<sup>2</sup>*Laboratoire Fluides, Automatique et Systèmes Thermiques, UMR No. 7608, CNRS, Universités Paris 6 and 11,*

*Bâtiment 502, Campus Paris Sud, 91405 Orsay Cedex, France.*

(Dated: January 30, 2022)

Tracer dispersion is studied experimentally in periodic or disordered arrays of beads in a capillary tube. Dispersion is measured from light absorption variations near the outlet following a steplike injection of dye at the inlet. Visualizations using dye and pure glycerol are also performed in similar geometries. Taylor dispersion is dominant both in an empty tube and for a periodic array of beads: the dispersivity  $l_d$  increases with the Péclet number  $Pe$  respectively as  $Pe$  and  $Pe^{0.82}$  and is larger by a factor of 8 in the second case. In a disordered packing of smaller beads (1/3 of the tube diameter) geometrical dispersion associated to the disorder of the flow field is dominant with a constant value of  $l_d$  reached at high Péclet numbers. The minimum dispersivity is slightly higher than in homogeneous nonconsolidated packings of small grains, likely due to heterogeneities resulting from wall effects. In a disordered packing with the same beads as in the periodic configuration,  $l_d$  is up to 20 times lower than in the latter and varies as  $Pe^\alpha$  with  $\alpha = 0.5$  or  $\alpha = 0.69$  (depending on the fluid viscosity). A simple model accounting for this latter result is suggested.

PACS numbers: 47.56.+r, 05.60.Cd

## I. INTRODUCTION

### A. Objectives of the paper

Understanding mass and solute transfer in porous and fractured media is relevant to many fields of science and engineering due to their applications in domains such as waste management and hydrology [1, 2, 3, 4]. A particularly sensitive method for characterizing mass transfer and detecting flow heterogeneities is the dispersion of a tracer in a flow of fluid through these media.

In homogeneous 3D porous media, the variation in the flow direction  $x$  of the concentration  $C$  of passive tracer is often observed to satisfy at a macroscopic scale (a few pore sizes) the classical convection-diffusion equation [1]:

$$\frac{\partial C}{\partial t} + U \frac{\partial C}{\partial x} = D_{\parallel} \frac{\partial^2 C}{\partial x^2} \quad (1)$$

Here,  $U$  is the flow velocity and  $D_{\parallel}$  is the dispersion coefficient measured in the flow direction and which characterizes the longitudinal spreading of the tracers during their transport.

In porous media, the dispersion coefficient is observed to be velocity dependent [3]. At a low velocity, molecular diffusion predominates and the dispersion coefficient is close to the molecular diffusion coefficient  $D_m$ . When the velocity increases, different regimes are observed and non trivial relations such as power law variations of the dispersion coefficient with the velocity are reported [5, 6, 7, 8, 9, 10]. The objective of the present paper is to report dispersion experiments on well controlled models consisting of beads placed inside a long capillary. Different ordered and disordered bead layouts

are considered and a rich variety of dispersion behaviors is observed.

### B. Key dispersion mechanisms

Two physical mechanisms cause the dispersion of passive tracers: molecular diffusion across and along streamlines and advection. Advection refers to tracer transport by the motion of the host fluid. In order to compare both mechanisms, it is useful to define the Péclet number:  $Pe = Ud/D_m$  where  $d$  is a characteristic length scale. In this work,  $d$  is either the bead or the tube diameter (the latter is used when the flow tube does not contain any beads).

In porous media, the void structure is complex, resulting in tortuous streamlines along which the velocity may greatly fluctuate. In randomly packed beads, for instance, current tubes often get split so that the fluid may flow around a bead; this results in variations of both the magnitude and the direction of the local velocity [11, 12]. With respect to the average flow, tracers therefore perform a random walk between pores characterized by the duration  $t \sim d/U$  of single steps where  $d$  is the bead diameter. Using this description, one expects a longitudinal dispersion coefficient  $D_{\parallel}/D_m \sim d^2/D_m t \sim Pe$  and a dispersivity,  $l_d = D_{\parallel}/U$ , constant and corresponding to the correlation length of the velocity field. Yet, regions of slow moving fluid, such as boundary layers, may also play a significant part and lead to logarithmic corrections [13].

In some specific configurations such as flow in a capillary tube [14, 15], in a periodic square array of beads [9, 16] or in a fracture [5, 6, 7], the velocity field has long range correlations. In such media, the flow velocity difference between the walls bounding the open space and

its center stretches the tracer front and creates concentration gradients: The latter are balanced by molecular diffusion across the gradient. In such a case, the typical time for the decorrelation of the tracer velocity is :  $t \sim d^2/D_m$  *i.e.* the characteristic time of molecular diffusion across the streamlines and the dispersion coefficient scales like  $D_{\parallel}/D_m \propto Pe^2$ . This regime is often called *Taylor dispersion* and, for flow in a capillary tube of inner diameter  $D$ , one finds [15]:

$$\frac{D_{\parallel}}{D_m} = 1 + \frac{Pe^2}{192}, \quad (2)$$

where  $Pe = UD/D_m$ . Equivalently, one can write :

$$\frac{l_d}{d} = \frac{1}{Pe} + \frac{Pe}{192}. \quad (3)$$

While periodic 3D porous media are very difficult to realize experimentally (even using perfectly monodisperse beads), the transition from Taylor to geometrical dispersion could be demonstrated numerically on 2D networks of increasing disorder [10].

Yet, some experiments on geological materials, either at the lab or field scales, display non Fickian characteristics. In these situations, the breakthrough curves observed are characterized by tails at long times. This effect may be explain either by the presence of heterogeneities at the scale of the sample or by the trapping of solute in microscopic dead ends or stagnant pores.

In this work, dispersion experiments in bead packings of varying degrees of disorder are reported. Depending on the structure of the packings, a variety of dispersion regimes is observed ranging from geometrical to Taylor dispersion and including intermediate regimes and non Fickian dispersion. From these experiments, the tube/bead diameter ratio appears as a key control parameter of the dispersion regime.

## II. EXPERIMENTAL SET-UP AND PROCEDURE

The experimental model used in this work closely resembles that used by Baudet and coworkers [17]. In this latter work, tracer dispersion was measured in a long capillary tube filled with monodisperse beads and with a tube/particle diameter ratio of the order of 1.25. The layout of the beads was either periodic or disordered. The first configuration was achieved by adding one by one beads in an horizontal capillary tube. Finally, one ends up with a line of beads, each of them being in contact with its two neighbors and with the tube wall. The second layout is obtained by tilting the capillary tubes while filling them. The beads fall then on top of each other and slide often sideways, resulting in a denser packing. The final packing is random and beads are added in the tube until it is entirely filled.

In this work, the inner diameter of the capillary tube

is  $D = 3.1 \pm 0.1$  mm, its length is 1500 mm and well calibrated stainless steel spheres of diameter  $d$  are used. Beads of diameter  $d = 2.54 \pm 0.02$  mm were chosen in order to reproduce the configuration used by Baudet *et al* [17]. In addition to these two bead packs, two more configurations were used (see Fig. 1). The first one uses the same tube but empty. In the last one, the diameter of the beads is  $d = 1 \pm 0.01$  mm, *i.e.* three time smaller than the tube diameter, leading to a larger tube-to-particle ratio. In order to clarify the present paper, the following convention is used :

- *(E) Empty channel*: the capillary tube is devoid of beads.
- *(O) Ordered channel*: the tube contains a periodic line of beads touching each other.
- *(DI) Disordered channel I*: the beads are still touching each other but build up a disordered array. The tube/bead diameter ratio is 1.22.
- *(DII) Disordered channel II*: the arrangement is of the same type as *(DI)* but the diameter of the beads is smaller  $d = 1 \pm 0.01$  mm. The tube/bead diameter ratio is 3.1.

In configurations (O) and (DI), the diameter of the spheres is slightly smaller than the tube diameter ( $d = 2.54 \pm 0.02$  mm). In configuration *(DII)*, the diameter of the beads is three times smaller than that of the tube ( $d = 1 \pm 0.01$  mm) Originally, one end of the capillary

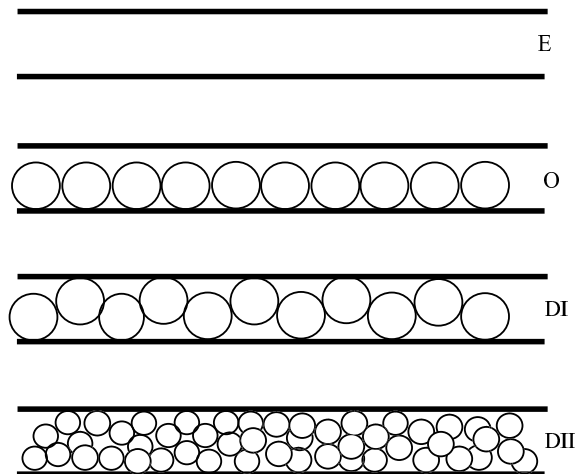


FIG. 1: Flow geometries used in the experiments. From top to bottom : Empty Channel - Ordered Channel - Disordered Channel I - Disordered Channel II.

tube is connected to a syringe pump allowing to establish a stationary flow of the transparent fluid through the channel: A valve allows to switch the injection to a dyed solution of identical properties. Fluid flowing out of the other end of the tube is weighed by computer controlled scales, allowing to measure the flow rate throughout the experiment.

The fluids used are solutions of either 10% or 70% of glycerol in water and their dynamic viscosities  $\mu$  are respectively  $1.3 \times 10^{-3}$  Pa.s and  $23 \times 10^{-3}$  Pa.s (at  $20^\circ\text{C}$ ). Water Blue dye at a concentration of 0.05 g/l is added to one of the solutions: It has been selected because it is chemically stable and does not modify the rheological properties of the solution. The molecular diffusion coefficient  $D_m$  of the dye was determined through independent Taylor dispersion measurements performed in a vertical teflon capillary tube. One obtains in this way  $D_m = 6.5 \cdot 10^{-4}$  mm<sup>2</sup>/s for the 10% glycerol solution; for the 70% solution, the value  $D_m = 3.25 \cdot 10^{-5}$  mm<sup>2</sup>/s is deduced from the value for the first solution by the Stokes-Einstein relation [18]. In the present experiments, the Péclet number ranges from 50 to  $10^4$  for the 10% glycerol solution but reaches  $1.4 \times 10^5$  for 70% glycerol solutions. In all the studies the Reynolds number is less than 1 except for the empty tube where  $Re$  can reach 10: Under such conditions, the flow can be considered as stationary [11].

In this work, the variation of the tracer concentration at the outlet with time, known as the breakthrough curve, is determined from light absorption by the dye. The measurement is realized over a square window of size 0.3 mm<sup>2</sup> located at 1450 mm from the injection, close to the outlet and immediately downstream of the last bead of the bed. In order to reduce optical distortion induced by the tube curvature, the measurement section is enclosed within a transparent plexiglas cell with flat parallel walls. The cell is originally filled with glycerol, a fluid with a refractive index close to that of the tube. The section of the tube inside this cell is inserted between a light panel and a 4096 gray levels CCD camera (Roper Coolsnap CF). The set-up is illuminated by a fluorescent tube placed on the opposite side from the camera and excited at a high frequency to reduce fluctuations. For each experiment, 2000 images are recorded by a computer connected to the camera at time intervals ranging from 1 to 30 sec depending on the flow rate. Dye concentration values are determined quantitatively using calibration measurements realized independently with the experimental tube saturated with dye solutions of different known concentrations. Finally, drifts of the light intensity are measured in a region of interest outside the tube; these measurements are then used during the analysis of the images to compensate for the effect of these variations on the transmitted light intensity in the experimental section.

Using this experimental procedure, breakthrough curves were measured for different flow velocities and for different bead layouts. The results of these global measurements are given and discussed in section III. Moreover, in order to improve interpretations of the breakthrough curves, visualizations realized independently at a local scale in a similar configuration were carried out. In these latter experiments, a transparent tube of  $D = 8$  mm inner diameter is filled with glass beads of diameters 6, 3 or 2 mm. These beads were chosen so that the

corresponding tube/bead diameter ratio is respectively 1.33, 2.67 and 4, close to the values used in the dispersion experiment. Originally, the model is saturated with glycerol (viscosity  $\simeq 1$  Pa.s) which is displaced by the same fluid but dyed. Using a fluid with such a high viscosity (and therefore a low diffusion coefficient) allows to observe and separate clearly the various flow paths at low Reynolds numbers inside the sample.

Before describing in detail the various dispersive regimes observed for the different bead layouts, the next section describes the methods used to determine the dispersion coefficients from the breakthrough curves.

### A. Analysis of experimental curves

Figure 2 displays a typical breakthrough curve obtained after a stepwise injection of the dyed fluid; asymmetrical curves were also obtained and their analysis will be discussed later. Under such initial conditions and if the concentration satisfies the classical convection-diffusion equation given by Eq. (1), the concentration variation at the outlet is given by:

$$\frac{C(L, t)}{C_0} = \frac{1}{2} \left( 1 - \operatorname{erf} \frac{L - Ut}{\sqrt{4D_{\parallel}t}} \right). \quad (4)$$

Where,  $C_0$  is the dye concentration in the displacing fluid,  $L$  the distance between the measurement section and the injection point,  $D_{\parallel}$  is the longitudinal dispersion coefficient,  $U$  is the mean flow velocity. The figure (2) shows the fit of the breakthrough curve by the function given by Eq. (4) where the only adjustable parameter is  $D_{\parallel}$ . The two curves are almost undistinguishable, indicating that the dispersion process is Fickian and that the classical convection-diffusion equation (1) is satisfied. Yet,

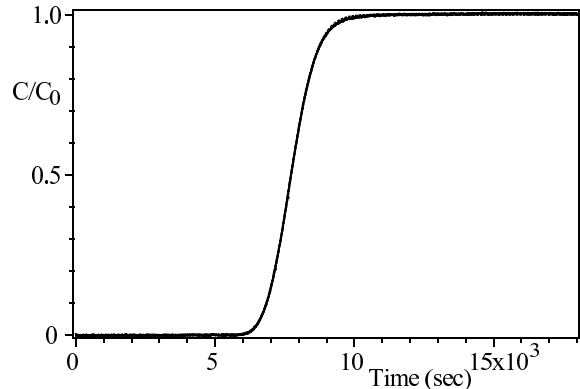


FIG. 2: Continuous line : typical tracer variation concentration as a function of time for a type  $DI-$  array and for  $Pe = 930$  (continuous line).- Dotted line : curve fitted with a variation from Eq. (4.)

such perfect fits were not always observed. For instance, in the  $O$  configuration and for fairly high velocities  $U$ , one observes at long times, as can be seen on Fig. 3, a

"tail" effect : it corresponds to an exponential relaxation of the concentration towards a limiting value with a typical time of the order of  $L/U$ . Such breakthrough curves are better fitted by solutions of the classical Coats-Smith capacitive model [19] which uses four fitting parameters:  $\bar{t} = L/U$ ,  $D_{\parallel}$ ,  $f$  and  $t_f$ . The two last parameters correspond to the amplitude and the characteristic time of the exponential variation in the "tail" at long times. By combining these parameters, one obtains an asymptotic dispersion coefficient  $D_{\parallel as}$  :

$$\frac{D_{\parallel as}}{D_m} = \frac{D_{\parallel}}{D_m} + (1-f)^2 U^2 t_f, \quad (5)$$

$D_{\parallel as}$  represents the value of the dispersion coefficient that would be measured for channels with the same local structure, but long enough so that a Gaussian dispersion regime is reached and Eq. (1) becomes valid. Note that the Coats-Smith model is only used here as a mathematical way of obtaining the value of  $D_{\parallel as}$ ; the fact that the experimental curves are well fitted by the model does not mean that its underlying assumptions are valid (namely the existence of a zero flow zone with an exponential exchange with the mean flow). In the following, the dispersivity  $l_d$  is taken equal to  $D_{\parallel as}/U$  only for experiments in the  $O$  configuration, in the other configurations,  $D_{\parallel}$  is obtained by fitting the experimental curves to Eq. (4).

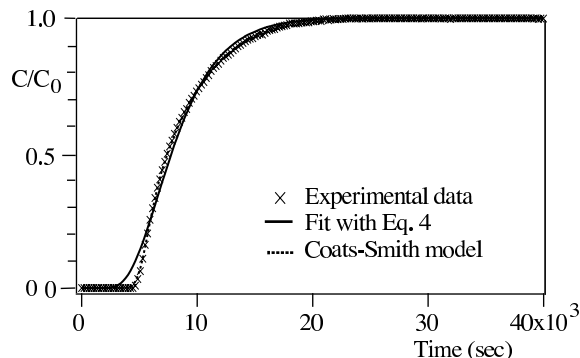


FIG. 3: Continuous line : experimental dye concentration variation as a function of time for an ordered  $O$ -type array of 2.54 mm diameter beads and for  $Pe = 1000$ . Dotted lines : Gaussian and Coats-Smith fits.

### III. EXPERIMENTAL RESULTS

Figure 4 displays variations of the dispersivity  $l_d$  as a function of the Péclet number measured for the different channel configurations used in the present work. Note that all the experiments were carried out twice: First, the dyed fluid was injected to displace the clear solution flowing initially in the model at the same flow rate. After the model has been completely saturated with the dyed fluid, it is displaced in a second experiment by the clear fluid, still at the same flow rate. The dispersion coefficient

was found to be identical in the two experiments, implying that no instabilities modified the flow.

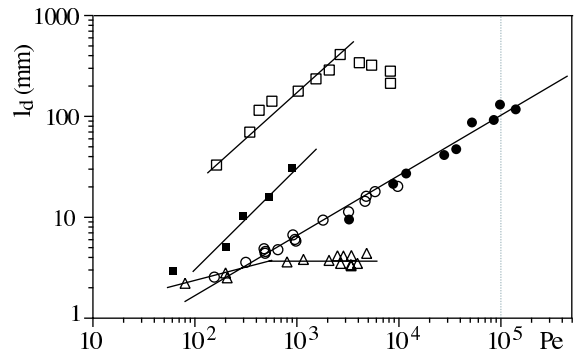


FIG. 4: Variation of the dispersivity  $l_d$  as a function of the Péclet number: ( $\Delta$ )  $DII$ -array; ( $\circ, \bullet$ )  $DI$ -array respectively for solutions of 10% and 70% glycerol in water; ( $\blacksquare$ )  $E$ -array; ( $\square$ )  $O$ -array (in this latter case  $l_d = D_{\parallel as}/U$ ).

#### A. Empty tube ( $E$ -Channel)

In the case of an empty tube, all the experimental dispersion curves are well adjusted by the concentration variation given by Eq. (4). The corresponding dispersivities  $l_d$ , as plotted in Figure 4, increase linearly with  $Pe$  reflecting, as expected from Eq. (3), a dominant influence of Taylor dispersion. One sees from Eq. (3) that the value of  $l_d$  is related to the tube diameter; a linear regression of the data gives indeed an effective value of the tube diameter :  $a_{eff} \simeq 3 \pm 0.2$  mm.

#### B. Ordered array of beads ( $O$ -Channel)

Dispersivity  $l_d$  values for the ordered array of beads plotted in Figure 4 were obtained with the Coats-Smith model. For  $Pe \leq 2500$ ,  $l_d$  varies with  $Pe$  following a power law :  $l_d \sim a_{eff} Pe^\alpha$  (straight line in log-log coordinates). From a regression over the experimental data, one obtains  $a_{eff} \simeq 0.6$  mm and  $\alpha = 0.85 \pm 0.2$ : This value is compatible with a Taylor dispersion mechanism for which  $\alpha = 1$ .

One can indeed expect that, in this channel, fluid particles follow streamlines determined by the periodic structure of the bed of beads: Therefore, as in capillary tubes, tracer can only move from a streamline to another through molecular diffusion (See Fig. 5). An important feature is the fact that the experimental values of  $l_d$  which vary from 40 mm to 400 mm are about 8 times larger than for the empty capillary tube at a same mean flow velocity. This cannot be explained by the partial filling up of the flow channel by the beads. On the opposite, since these reduce the effective aperture of the flow channels,  $l_d$  should drop off following Eq.(3) which is not observed.

Direct visualizations realized in a similar periodic geometry (Figure 5), although with larger beads, help understand these results: Pure glycerol is used in these experiments to visualize clearly the boundaries between fluids by removing the influence of molecular diffusion. In

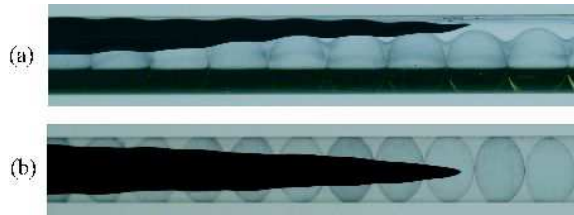


FIG. 5: Miscible displacement of pure by dyed glycerol in an ordered array of beads inside a capillary tube : (a) side view (b) top view (bead diameter :  $d = 6$  mm; tube diameter :  $D = 8$  mm)

this figure, one observes that the dyed fluid displays a tongue like structure and wraps around the beads. This shape shows that the streamlines are mostly oriented in the flow direction with tiny undulations induced by the beads. Another important point is that the dyed fluid does not flow in the narrow space between the beads: Mass transfert between the two regions can thus only occur through molecular diffusion. This explains the long tail observed in the breakthrough curves. Finally, the tongue-like structure reveals the strong velocity contrast between the fluid flow on the side of the beads and above them. The velocity gradient stretches the tracer fronts resulting in a concentration gradient which, in turn, gets smoothed by a transverse diffusive flux.

All ingredients of a Taylor like dispersion regime are thus present. Yet, because of the beads, the diffusive flux is more tortuous than in an empty capillary tube: Tracer has to flow around the beads to reach the outlet of the tube. The time needed to homogenize the tracer concentration in the tube section is thus longer, resulting in a higher dispersivity.

At the highest flow velocities, the variation of  $l_d$  levels off and it starts to decrease. A possible explanation is the fact that, in this range of  $Pe$  values, the Reynolds number becomes higher than 1 ( $Re > 5$ ): recirculation flows may then develop and induce a more efficient transverse mixing than molecular diffusion. This may account for the decreasing value of  $l_d$  at high Péclet numbers.

### C. Disordered array of small beads (*DII*-array)

For a disordered array of 1 mm diameter beads inside the tube, the dispersivity  $l_d$  increases slowly as a function of  $Pe$  before reaching a constant value of the order of 3 mm for  $Pe \gtrsim 600$ . This constant limiting value of  $l_d$  implies that geometrical dispersion associated with the random velocity variations from one pore to the next is dominant. Also, in such geometries, the correlation

length of the velocities of fluid particles along their path is too short for Taylor dispersion to have a significant influence. Dispersion characteristics of such arrays are then comparable to those of non consolidated packings of monodisperse grains: In this latter case, the minimum value of  $l_d$  is lower than the grain size (typ.  $0.6 - 0.7 d_g$ ) and is reached for Péclet numbers (based on the grain size) of the order of 10 [20]. In Fig. 4, the value of  $l_d$  for a similar Péclet number ( $Pe = 30$  when based on the tube diameter) is  $l_d = 2$  mm or about twice the bead diameter. This result also suggests that boundary layers have a weaker influence on dispersion than predicted by some theories [13] since no increase of  $l_d$  as  $\text{Log}Pe$  is observed.

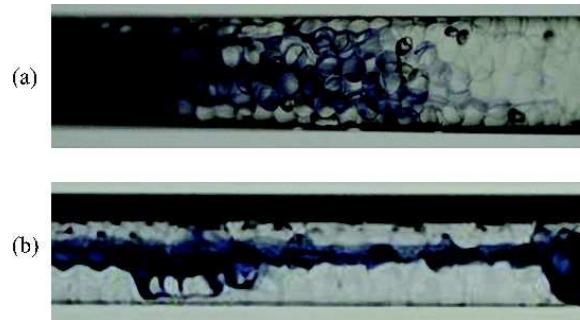


FIG. 6: Miscible displacements of pure glycerol by dyed glycerol saturating disordered glass beads packings inside a  $D = 8$  mm diameter capillary tube. Bead diameter : (a)  $d = 2$  mm - (b)  $d = 3$  mm. The tube/particle diameter ratio is respectively 4 and 2.66.

Visualizations realized with  $d = 2$  and 3 mm beads inside a  $D = 8$  mm diameter tube (Figs 6a-b) help understand these results. Figure 6a demonstrates clearly the many divisions of the front of injected fluid after moving through several pores and the rather uniform distribution of the invading fluid across the flow section : for the less viscous fluids used in our dispersion experiments, transverse molecular diffusion would mix quickly these thin filaments with the surrounding fluid, leading to the Gaussian dispersion observed for the *DII*- array.

For the lower value 2.66 of the ratio  $d/D$  the shape of the dye streaks changes very much as shown on Figure 6b. In this particular case, flow is strongly channelized in the center of the column; this indicates, that for some (low) values of the ratio  $d/D$ , pathological structures of the flow field may appear. The dispersion measurements reported in the present section were performed with a column for which  $d/D$  was intermediate between the two values in Figs. 6a-b. Since no channelization of the flow was observed visually during the measurement, the geometrical dispersion observed corresponds most likely to the type of flow structure shown in Fig.6a. In the next section, tracer dispersion is investigated for still smaller values of  $d/D$ .

#### D. Disordered array of large beads (*DI*-array)

In this case, the beads have the same diameter as in the periodic *O*-channel (i.e.  $d = 2.54$  mm), but the packing is now disordered (See Fig. 1). The experiments were performed using the two water-glycerol solutions containing either 10% or 70% of glycerol in weight. As for the *DII* array and in contrast with the ordered one, all breakthrough curves are well adjusted by Eq. (4) allowing for the determination of  $D_{\parallel}$  for the various flow conditions. The Figure 4 shows the dispersivity  $l_d = D_{\parallel}/U$  as a function of the Péclet number for the two solutions used in the experiments.

Clearly, the dispersivity  $l_d$  and  $Pe$  have a power law relationship. Fitting the variation of  $l_d$  with  $Pe$  to  $a_{eff}Pe^{\alpha}$  gives respectively for the 10% and 70% glycerol solutions  $\alpha = 0.52 \pm 0.01$ ,  $a_{eff} \simeq 0.2$  mm and  $\alpha = 0.69 \pm 0.04$ ,  $a_{eff} \simeq 0.04$  mm. One observes that  $a_{eff}$  and  $\alpha$  are only slightly different for the two solutions despite a ratio of 20 between the viscosities. One notices that the values of  $l_d$  for a given Péclet number are much lower for the disordered array than for the periodic one (by a factor of 15 (resp. 40 at low (resp. high)  $Pe$  values). Also, at low Péclet numbers,  $l_d$  becomes of the order of the bead size and gets close to the dispersivity observed for the *DII* array.

An important feature is the fact that the exponent  $\alpha$  characterizing the variation of  $l_d$  with  $Pe$  is of the order of 0.5 (for the 10% solution) and of 0.69 for the other one (at slightly higher Péclet numbers). These exponents are intermediate between the values  $0.82 \pm 0.2$  for the periodic array and 1 for the empty tube and the value 0 (constant  $l_d$ ) for the disordered packing of smaller beads: This implies that the dispersion mechanism is intermediate between Taylor and geometrical dispersion corresponding respectively to the first and second cases. This result was also observed by Baudet *et al* [17] but remained unexplained.

As in the previous sections, visualization on a larger system with the same  $d/D$  ratio help understand the dispersion mechanisms. The visualizations of Figure 7a-b show that the dyed fluid is mostly split into two streaks located near the walls. This channelization results from the increase of the porosity near the walls [22]; moreover, the low value of the tube/bead diameter ratio (of the order of 1) breaks the angular isotropy of the porous structure and concentrates the flow paths in a few (here 2) channels. Magnico [12] estimated that, at low Reynolds numbers, a fluid layer of thickness of the order of  $d/4$  appears, inside which fluid flow is purely longitudinal and tangential with no radial component. At first, one expects therefore radial exchange between the dye streaks, clearly visible on Figure 7a, and the remaining pore space to be mostly diffusional. Yet, as can be seen of the Figure 7b structural heterogeneity resulting from misplaced beads split the streaks into filaments parallel to the mean flow [11]; the number of filaments increases then along the flow path and their size decreases. These filaments

persist over distances significantly larger than the bead diameter so that molecular diffusion may spread the filaments over transverse distances of the order of their size. This gives rise to Taylor-like dispersion so that the global dispersion results from the combined influences of geometrical and Taylor dispersions. Such an influence of the flow channelization on dispersion was recently reported by Bruderer *et al* [10] in 2D networks.

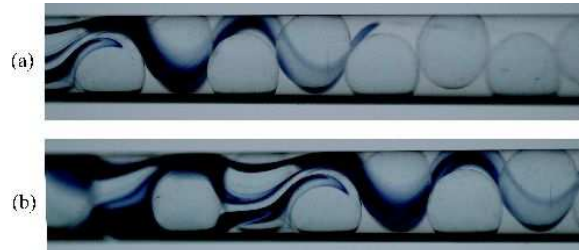


FIG. 7: Views at different times of the miscible displacement front of pure by dyed glycerol in a disordered channel: the diameter of the beads is  $d = 6$  mm and the diameter of the tube  $D = 8$  mm. The tube-to-particle ratio is 1.33.

#### E. Qualitative model of different power law variations

A qualitative argument helps understand how one can reach such power law variations of  $l_d \propto Pe^{\alpha}$  ( $0 < \alpha < 1$ ) under the combined influence of the disorder of the flow field and of transverse molecular diffusion. Assume that the front gets divided into streaks of width  $a_x$  decreasing with the distance  $x$  parallel to the flow as  $a_x \sim d^{1+\beta}x^{-\beta}$  (the  $d$  term allows to have the right dimensionality for the equation). By generalizing the Taylor argument, the transition to diffusive spreading should occur when the transverse molecular diffusion time  $\tau_{diff}$  across the distance  $a_x$  is of the order of the mean transit time  $L/U$  with :

$$\tau_{diff} \sim \frac{a_x^2}{D_m} \sim \frac{x}{U} \quad (6)$$

Replacing  $a_x$  by its expression provides the distance at which the transition should take place :

$$x_{trans} \sim d \left( \frac{Ud}{D_m} \right)^{1/(1+2\beta)} \sim dPe^{1/(1+2\beta)} \quad (7)$$

With, as usual,  $Pe = Ud/D_m$ . As in Taylor dispersion,  $x_{trans}$ , represents the characteristic decorrelation distance of the velocity of tracer particles and we assume therefore that  $D_{\parallel} \sim Ux_{trans}$  leading to

$$D_{\parallel eff} \sim UdPe^{1/(1+2\beta)} \quad (8)$$

or

$$\frac{D_{\parallel eff}}{D_m} \sim Pe^{\frac{2+2\beta}{1+2\beta}} \quad (9)$$

For  $\beta = 0$  (no geometrical variation of the filament width with distance), one retrieves Taylor dispersion with  $D_{\parallel Taylor} \sim a^2 U^2 / D_m$  and for  $\beta = \infty$  (fast decorrelation), one obtains geometrical dispersion with  $D_{\parallel geom} \sim dU$  (the exponent  $\alpha$  defined previously should then be related to  $\beta$  by  $\alpha = 1/(1 + 2\beta)$ ). In the present case, the experimental result  $D_{\parallel} \propto Pe^{3/2}$  implies that  $\beta = 1/2$ . Therefore, the experimental observations on  $DI-$  may be accounted for by assuming a combination of the influences of transverse molecular diffusion and of the geometrical disorder of the packing with, for the latter, a rate of division of the fluid streaks intermediate between those observed in a packing of small beads and in a capillary tube.

#### IV. CONCLUSION

To conclude, despite its simple structure (a long tube filled up with beads), the experimental system studied in the present work displayed a broad variety dispersion regimes. Both the layout of the beads and the ratio of their diameter to that of the tube were shown to influence very much the dispersion characteristics. First, Taylor dispersion is observed for a periodic bead array inside a tube of slightly larger diameter than the beads, like in the empty tube but with an increased dispersion coefficient. With the same beads inside the same tube, but packed in a disordered array, the dispersivity  $l_d$  is very strongly reduced and the exponent  $\alpha$  characterizing the variation of  $l_d$  with  $Pe$  decreases

from almost 1 to 0.5. This variation reflects the reduced persistence length of fluid streaks as they move along the tube (this length remains however much larger than the bead diameter). A simple model assuming a power law reduction of the width of the streaks of dye with distance allows to reproduce this variation of  $l_d$  with  $Pe$ . When the ratio of the tube and particle diameters is increased by using beads of smaller diameter, the dispersion coefficient varies with the Péclet number as  $D_{\parallel} \propto Pe$  for  $Pe > 600$ . This reflects a geometrical dispersion regime with a short persistence of the dye streaks controlled by the local pore geometry and a weak influence of diffusion in the boundary layers.

More observations of the flow and concentration fields at the local scale (using for instance matched index fluids) are needed to explain *quantitatively* these results. The increase of the dispersivity for the periodic array compared to the empty tube and the decorrelation of the motions of the fluid particles in the disordered arrays for small tube/particle diameter ratios are two particularly important issues.

#### Acknowledgments

We thank J. Koplik and G. Drazer for very helpful comments and discussions. This work was supported by UBA-*IN029*, CNRS-Conicet International Cooperation Program (PICS  $N^\circ$  2178) and by the ECOS Sud program  $N^\circ$  A03E02.

- 
- [1] J. Bear, *Dynamics of Fluids in Porous Media*, Dover Publications, New York (1988).
  - [2] F.A.L. Dullien, *Porous media, fluid transport and pore structure*, 2nd ed., Academic Press, New York (1991).
  - [3] J. Bear, C.-F. Tsang and G. de Marsilly eds., *Flow and Contaminant Transport in Fractured Rock*, Acad. Press (1993).
  - [4] M. Sahimi *Flow and Transport in Porous Media and Fractured Rocks : From Classical Methods to Modern Approaches*, John Wiley and Sons (2005).
  - [5] I. Ippolito, G. Daccord, E.J. Hinch and J.P. Hulin, J. Contaminant Hydrology **16**, 87 (1994).
  - [6] R.L. Detwiler, H. Rajaram and R.J. Glass, Water Resour. Res. **36**, **1611** (2000).
  - [7] A. Boschan, H. Auradou, I. Ippolito, R. Chertcoff, and J.P. Hulin submitted to Water Resour. Res. (2006).
  - [8] J.D. Seymour and P.T. Callaghan, AIChE J. **43**, 2096 (1997).
  - [9] R. S. Maier, D. M. Kroll, R. S. Bernard, S. E. Howington, J. F. Peters and H. T. Davis, Physics of Fluids **12** 2065 (2000).
  - [10] C. Bruderer and Y. Bernabé, Water Resour. Res. **37**, 897 (2001).
  - [11] T. H. Wegner, A. J. Karabelas and T. J. Hanratty, Chem. Eng. Sci. **26**, 59 (1971).
  - [12] P. Magnico, Chem. Eng. Sci. **58**, 5005 (2003).
  - [13] D.L. Koch and J.F. Brady, J. Fluid Mech. **154**, 399 (1985).
  - [14] G. I. Taylor, Proc. Roy. Soc. London A **219**, 186 (1953).
  - [15] R. Aris, Proc. Roy. Soc. London A **235**, 67 (1956).
  - [16] J. Salles, J.-F. Thovert, R. Delannay, L. Prevors, J.-L. Auriault and P.M. Adler, Phys. Fluids A **5**, 2348 (1993).
  - [17] C. Baudet, R. Chertcoff and J-P. Hulin, C. R. Acad. Sci. Paris, II, **305**, 20 (1987).
  - [18] W.B. Russel, D.A. Saville, and W.R. Schowalter, Colloidal Dispersions Cambridge University Press, Cambridge, UK, Chapter 3 (1995).
  - [19] K. H. Coats and B. D. Smith, Soc. Pet. Eng. J. Trans. AIME **231**, 73 (1964).
  - [20] N-W. Han, J. Bhakta and R.G. Carbonell, AIChE **31**, 277 (1985);
  - [21] D.L. Koch, R.G. Cox, H. Brenner, and J.F. Brady, J. Fluid Mech. **200**, 173 (1989).
  - [22] G. E. Mueller, Powder Technology **72**, 269 (1992).